HHS Public Access

Author manuscript

Am J Transplant. Author manuscript; available in PMC 2017 June 01.

Published in final edited form as:

Am J Transplant. 2016 June ; 16(6): 1726–1738. doi:10.1111/ajt.13688.

Antibody mediated rejection in sensitized non-human primates: modeling human biology

Christopher K. Burghuber[1,2], **Jean Kwun**[1,3], **Eugenia J Page**[1], **Miriam Manook**[3], **Adriana C Gibby**[1], **Frank V Leopardi**[1,3], **Minqing Song**[1,3], **Alton B Farris III**[4], **Jung Joo Hong**[4,5,6], **Francois Villinger**[4,5], **Andrew B. Adams**[1], **Neal N Iwakoshi**[1], and **Stuart J Knechtle**[1,3,*]

[1]Emory Transplant Center, Department of Surgery, Emory School of Medicine, Atlanta, Georgia

[2]Division of Transplantation, Department of Surgery, Medical University of Vienna, Vienna, Austria

[3]Duke Transplant Center, Department of Surgery, Duke University, Durham, North Carolina

[4]Department of Pathology, Emory School of Medicine, Atlanta, Georgia

[5]Division of Microbiology and Immunology, Yerkes National Primate Research Center, Emory University, Atlanta, Georgia

[6]National Primate Research Center (NPRC), Korea Research Institute of Bioscience and Biotechnology (KRIBB), Ochang, Korea

Abstract

We have established a model of sensitization in non-human primates and tested two immunosuppressive regimens. Animals underwent fully mismatched skin transplantation, donor-specific antibody (DSA) response was monitored by flow crossmatch. Sensitized animals subsequently underwent kidney transplantation from their skin donor. Immunosuppression included tacrolimus, mycophenolate and methylprednisolone. Three animals received basiliximab induction, compared to non-sensitized animals they showed a shorter mean survival time (MST, 4.7±3.1 vs. 187±88 days). Six animals were treated with T-cell depletion (anti-CD4/CD8 mAbs), which prolonged survival (MST=21.6±19.0 days). All pre-sensitized animals showed antibody-mediated rejection (AMR). In 2/3 basiliximab animals cellular rejection (ACR) was prominent. After T cell depletion, 3/6 monkeys experienced early acute rejection within 8 days with histological evidence of thrombotic microangiopathy and AMR. The remaining three survived 27 to 44 days, with mixed AMR and ACR. Most T-cell depleted animals experienced a rebound of DSA that correlated with deteriorating kidney function. We also found an increase in proliferating memory B cells ($CD20^+CD27^+IgD^-Ki67^+$), lymph node follicular helper T cells ($ICOS^+PD\text{-}1^{hi}CXCR5^+CD4^+$) and germinal center response. Depletion controlled cell-mediated rejection in sensitized non-human primates better than basiliximab, yet grafts were rejected with concomitant DSA rise. This model provides an opportunity to test novel desensitization strategies.

[*]**Address all correspondence and requests for reprints to:** Stuart J Knechtle, ; Email: stuart.knechtle@dm.duke.edu.

Disclosure

The authors of this manuscript have no conflicts of interest to disclose as described by the American Journal of Transplantation.

Introduction

Sensitization is a critical problem in transplantation. Up to a third of patients on the kidney waiting list harbor antibodies against non-self antigens of the Major Histocompatibility Complex (MHC), called Human Leukocyte Antigens (HLA) (1, 2). In the U.S., HLA-sensitized patients face a significantly lower chance of receiving a transplant, compared to unsensitized patients (3). Recent changes to the deceased donor allocation system, and adoption of the Kidney Donor Profile Index (KDPI) have attempted to address this problem (4, 5). For patients with a living donor, paired donor kidney exchange is designed to circumvent HLA-incompatible transplantation. However, less than 2% of highly sensitized (cPRA>80%) patients benefit from such programs per year, despite being over-represented within the pool (1). For many U.S. patients, desensitization strategies with an incompatible living donor increase survival compared to waiting for an acceptable match (6). However, transplantation after desensitization increases the likelihood of both early and late antibody mediated graft loss (7, 8).

To date, desensitization strategies in transplantation have been almost exclusively based on antibody removal by plasmapheresis (PP) and immunoadsorption (IA; outside the U.S.) inactivation by intravenous immunoglobulin (IVIg; low or high dose), and B cell depletion with Rituximab. PP, IA and IVIg mainly target circulating alloantibody and although graft survival outcomes have been encouraging, AMR rates remain significant. Attempts to target B cells using Rituximab and splenectomy in addition to PP, IA and IVIG, benefit early graft survival, but do not reduce graft loss after the first year (9, 10). These methods of desensitization appear to be unable to ensure durable reduction of DSA, and rebound antibody production occurs post-transplant (11).

Investigating alternative strategies for desensitization in human patients is difficult, given the precious nature of donor organs. Small animal & xenotransplantantation models of sensitization rarely provide data that is directly applicable to clinical settings, as a result of inherently different MHC antigen expression, and immune response, as well as difficulties administering and monitoring multi-drug regimens (12). We therefore wanted to establish a large animal model in which to test the safety and efficacy of new therapies not yet used in clinical practice as well as to more rigorously study the mechanistic effects of drugs targeting antibodies, B cells, and plasma cells. In doing so, it was imperative to ensure that we could ensure the following: firstly, sustained development of donor specific antibody (DSA) pretransplant; secondly, use of clinically relevant induction therapies and thirdly, immunological and histological phenotypes that correlate with human sensitized recipients experiencing AMR.

We report our experience in the development of a sensitized rhesus macaque model of renal transplantation. After ensuring generation of significant levels of DSA, we employed clinically relevant induction therapies in these sensitized recipients and discovered distinct patterns of acute antibody-mediated injury that correlate with progressive changes in serology and immune repertoire.

Materials and Methods

Animal selection and care

All experiments were performed complying with the principles set forth in "The Guide for the Care and Use of Laboratory Animals", Institute for Laboratory Animal Research, National Academies of Sciences, Engineering and Medicine, Washington, DC. We obtained specific pathogen-free, 3 to 6 year old male rhesus macaques *(Macaca mulatta)* from Alpha Genesis Inc. (Yemassee, SC). Rhesus macaques were MHC genotyped by deep sequencing at the Genetics Services Unit, Wisconsin National Primate Research Center, Madison, WI. Donor-recipient pairs were selected by choosing maximal disparity for MHC class I & II. All medication and procedures were conducted in accordance with Yerkes National Primate Center, (Atlanta, GA) and the National Institutes of Health (Bethesda, MD) guidelines after approval by the Emory University Institutional Animal Care and Use Committee (Atlanta, GA).

Sensitization by skin grafting, kidney transplantation, clinical, graft and immune monitoring

Full-thickness abdominal skin grafts (~1 inch diameter) were exchanged between donor-recipient pairs, and secured on their dorsal skin with 4-0 nylon, adhesive bandage, and jackets (Lomir Biomedical, Malone, NY) for 7 days. Skin graft survival was evaluated on day 7 and/or whenever the animal was accessed. DSA, as measured by flow crossmatch, decreased over time (Figure 1C), therefore two sequential skin grafts were used in some animals to reliably sustain a positive flow crossmatch in the pretransplant period. After DSA levels stabilized, life-sustaining kidney transplantation was performed by simultaneous bilateral native nephrectomy, kidney exchange between donor-recipient pairs and implant using standard microvascular techniques. Peripheral blood was obtained weekly for complete blood counts, serum chemistry and tacrolimus trough levels. Real-time PCR was performed to measure rhesus cytomegalovirus (rhCMV) reactivation. Blood, bone marrow and axillary and/or inguinal lymph nodes were procured and used for flow cytometry. Graft biopsies were taken for indications such as rise in serum creatinine (sCr) or blood urea nitrogen (BUN) or decrease in urine output. Terminal kidney failure was defined by a prolonged rise of sCr > 4mg/dl and/or BUN > 80mg/dl, thereafter the animal was sacrificed and blood and tissues were procured. A group of 8 non-sensitized monkeys (NSENS-group) from an ongoing study at our center was used to compare survival with our first treatment group (BAS-group). These animals were matched and kidneys transplanted applying the same principles but did not undergo sensitization with skin transplantation.

Immunosuppressive and antiviral agents (see Figures 2A and 3A for dosing; see supporting information for dosing, brand names and providers)

Four transplant animals (monkeys #1–4) each received one skin graft. At kidney transplantation, induction with intravenous (IV) basiliximab was used (BAS-group) on the day of transplant and postoperative day (POD) 4; methylprednisolone was infused IV and

Supporting information
Additional Supporting Information may be found in the online version of this article.

subsequently tapered daily with intramuscular (IM) doses. Maintenance immunosuppression included tacrolimus IM (target trough level of 8–12ng/ml) and oral mycophenolate mofetil. Ganciclovir was given for prophylaxis and therapy of rhCMV reactivation. One animal (#2) succumbed to kidney failure on postoperative day (POD) 1 unrelated to rejection and was excluded from further analysis. NSENS-group monkeys received the same induction and maintenance immunosuppression as BAS-animals. Furthermore seven transplant animals (monkeys #5–11; DEPL-group) received two skin grafts prior to transplantation. Depleting rhesus anti-CD4 mAb (clone CD4R1) was administered 5 days before (D-5) and depleting rhesus anti-CD8 mAb (clone MT807R1) on the day of kidney transplantation (D0). Since anti-CD4 mAb activity was dependent on NK-cells, it was infused 5 days prior to NK-cell depleting anti-CD8 mAb. Maintenance immunosuppression was identical to the one used in the BAS-group. One animal (#7) succumbed to kidney failure on POD 3 unrelated to rejection and was excluded from further analysis.

Detection of donor-specific antibodies (DSA)

Alloantibody production was assessed retrospectively by flow cytometry crossmatch (FXM) of donor peripheral blood mononuclear cells (PBMC) or splenocytes with serially collected recipient serum samples. We incubated 3×10^5 donor PBMC with diluted recipient serum, washed and subsequently stained with anti-CD20, anti-CD3 and anti-monkey IgG (see supporting information for clones and providers). Individual runs by the same technician were performed according to a strictly standardized protocol using the same reagents, settings and flow cytometer. Crossmatch positivity, and hence ‘successful sensitization’ was defined by a twofold increase of mean fluorescence intensity (MFI) from pre-skin-transplant levels (MFI ratio ≥2). For analysis T cell crossmatches (TFXM) representing MHC class I antibodies were favored. Depleting CD4R1 mAb interfered with our secondary antibody such that post-transplant, BFXM only was analyzed.

Polychromatic flow cytometric analysis

Cells were stained with Live/Dead Fixable Aqua dead cell stain kit (Life Technologies, Grand Island, NY) and then with the following antibodies: monoclonal antibodies (mAb) against human CD3, CD4, CD8, CD20, CD25, CD27, CD28, CD56, CD95, PD-1, CXCR5, ICOS, NKG2a, CD14, IgD and after fixation Ki67 and FoxP3 (see supporting information for clones and providers). Samples were collected with a LSRII flow cytometer (BD Biosciences, San Jose, CA) and analyzed using FlowJo software vX (Tree Star, Ashland, OR).

Histology, immunohistochemistry and electron microscopy

All procedures were performed at the Emory Transplant Center or Yerkes National Primate Center Division of Pathology as described in (13). Briefly, tissue samples were fixed in formalin and embedded in paraffin. Hematoxylin and eosin (H&E), periodic acid Schiff (PAS), Masson’s trichrome stains and immunohistochemistry using a polyclonal anti-human-C4d (American Research Products, Waltham, MA) were obtained following center protocol (see supporting information for detailed description of germinal center staining and electron microscopy). A renal pathology specialist assessed histology in a blinded fashion adopting the current human Banff scoring system (14).

Statistical analysis

All data are presented as mean ± standard deviation (error bars in graphs) or as otherwise indicated. Sample comparisons of different animals and/or time points were achieved by two-tailed (paired) t-test in normally distributed data. In case of unequal variances we used Welch's t-test (15). One-way ANOVA with Dunnett's test was used comparing multiple time points to baseline. For survival analysis we used the Kaplan-Meier method and log-rank test. For within subject correlation of measurements we used a linear model with a random intercept to account for differences between subjects, modified from Bland JM, Altman DG (16). Values of $p<0.05$ were considered to be statistically significant. We used Prism 6.0 (GraphPad Software, San Diego, CA) and SPSS 21 (IBM Corporation, Armonk, NY).

Results

Sensitization of rhesus macaques through skin transplantation

The first aim of the model, was to show successful sensitization and generation of an alloimmune response. Fully mismatched skin grafts were used to sensitize rhesus macaques, and sensitization was confirmed using FXM testing. Sequential skin grafts were separated by a minimum 4-week interval in order to allow for fully mature memory B cell and plasma cell formation. All primary skin grafts were rejected within 14 days (Figure 1B). Anti-donor IgG antibodies were detectable in recipient sera at 2 weeks and peaked at approximately 6 weeks post–skin-transplant. Analysis of DSA using T cell flow crossmatch (TFXM), showed highly variable peak levels (MFI ratio 2.2 to 63.8, mean 13.6 ±15.6), B-cell flow cross match (BFXM) showed less variability (MFI ratio 2.4 to 13.4, mean 6.6 ±3.4) (Figure 1C).

Consistent with successful primary alloimmunization, the anamnestic response toward a second skin graft showed a faster response. All second skin grafts were rejected within 8 days (Figure 1B). DSA showed a rise, which was detectable at 1 week, reaching a peak at week 3. Successful sensitization according to our criteria (see methods) was always reached: TFXM MFI-ratio 10.2 to 75.1 (mean 35.3 ±17.4), BFXM MFI-ratios 8.5 to 45.5 (mean 20.1 ±11.6) (Figure 1C). The DSA level gradually declined after 10–12 weeks, despite this, antibody levels were sufficient to maintain a positive FXCM for over 30 weeks. These data suggest that skin transplantation induces sensitization and, after a second skin transplant, a durable and measurable DSA level is maintained.

Basiliximab induction therapy in sensitized non-human primates

In order to confirm the effect of sensitization induced by skin transplantation, we subjected three animals with a single skin allograft to life-sustaining kidney transplantation from their skin donors using basiliximab induction (BAS-group) with standard immunosuppression at least 140 days after initial sensitization (Figure 2, Table 1). Preoperatively the mean T and B cell MFI ratios were 2.70±1.31 and 2.66±1.33 respectively. All animals produced detectable amounts of urine after reperfusion. All three were sacrificed with clinical and laboratory signs of kidney dysfunction at post-operative days (POD) 2, 4 and 8 (animals #4, #1 and #3 respectively); the mean survival time (MST) was 4.67±3.1 days (Figure 2B). We compared this to a control group of eight monkeys that were not sensitized and received the same immunosuppression after kidney transplantation (NSENS-group). Mean survival time of this

cohort was 187±88 days, which was significantly different from the BAS-group (t-test p=0.0072). Graft histology was graded using Banff criteria (14), (Table 1). Among the diagnoses listed, glomerulitis (g), peritubular capillaritis (ptc) and C4d deposition are commonly seen with antibody-mediated rejection (AMR). Therefore the scores g + ptc + C4d were added to represent an antibody-mediated injury score. Evaluation of monkey #4, #1, and #3 with scores of 2, 6 and 6 respectively suggested antibody mediated injury in all three animals. Monkey #4's graft was suspicious for AMR as moderate glomerulitis was paired with focally prominent neutrophils and mononuclear cells in less than 10% of peritubular capillaries (PTCs). Monkeys #1 and #3 additionally displayed prominent features of cellular rejection including cellular infiltrate in the interstitium, arteritis (Supplemental Figure 1) and tubulitis and were classified as mixed AMR and ACR, the cellular portion corresponding to Banff scores of IIA and III respectively. While monkey #4's graft was negative for C4d staining the latter two showed minimal and focal (C4d1 and 2) positivity (Figure 2C). All grafts showed neutrophils and mononuclear cells in glomeruli and PTCs, monkeys #1 and 3 additionally displayed "activated" mononuclear cells as defined by the Cooperative Clinical Trials in Transplantation score system (17). The latter two were found to also harbor these cell types abundantly in graft interstitium in addition to plasma cells. Significantly accelerated graft rejection suggests that single skin allografts successfully sensitize recipients.

T-cell depletional therapy in sensitized non-human primates

Next, we used a T-cell depletion (novel anti-rhesus CD4 and CD8 T-cell) induction therapy as an alternative to basiliximab (DEPL-group, Figure 3A). The addition of a second skin graft reduced variability in measured DSA levels. Using this induction therapy, we subjected 6 animals to life-sustaining kidney transplantation at least 68 days after a second skin graft. Preoperatively the mean T and B cell FXM were 9.86±7.22 and 7.95±3.97 (MFI ratio) respectively (compared to the BAS-group there was no statistical difference in pre-operative T or BFXM: t-test p=0.14 and p=0.06). Maintenance immunosuppressive therapy was identical to the BAS-group. T-cell depletion was monitored by flow cytometry and showed a significant reduction of total lymphocytes, $CD3^+$, $CD4^+$, $CD8^+$ lymphocytes and NK cells defined as $NKG2a^+CD3^-CD14^-CD20^-$ mononuclear cells (18–20), measured within the first week after transplant (Figure 3B). Despite higher pre-operative DSA levels, DEPL animals had a tendency to survive longer than animals of the BAS-group (MST 21.67 ±19.0 vs. 4.67 ±3.1 days, log-rank test p=0.16; Figure 3C).

Interestingly, the cohort exhibited distinct kinetics of rejection that could be divided into either early or intermediate (Table 2). The early rejecting group experienced renal allograft failure within 8 days (monkeys #6, 8 and 11). Monkey #6 was anuric on POD1, color Doppler ultrasound found the perfusion in the renal periphery severely compromised. After necropsy, histologic examination of the macroscopically hemorrhagic graft revealed inflammatory cells in PTCs and glomeruli, necrosis and hemorrhage as well as fibrin deposition in glomeruli, capillaries and arterioles. C4d staining was positive and electron microscopy showed dilated PTCs and destruction of capillary walls. These findings were considered to be compatible with hyperacute rejection (Figure 4). Monkeys #8 and #11 showed severe thrombotic microangiopathy (TMA) with discrete thrombi in glomeruli and

PTCs accompanied by mild interstitial inflammation. There was no histological evidence of cellular rejection. Immunohistochemistry revealed focal C4d staining in PTCs (Figure 3D). Graft AMR scores were 6, 5 and 6 respectively. Neutrophils, mononuclear and activated mononuclear cells (17) were found in glomeruli of all three grafts and in PTCs of two grafts.

The intermediate group exhibited graft survival of up to 44 days (monkeys #5, #9 and #10). Graft histology displayed more interstitial inflammation as defined by Banff (i-scores 2, 1 and 2 respectively vs. 0 in all early rejectors), and C4d-staining was focal or diffuse (C4d2 or 3). Graft AMR scores were 6, 7 and 6, respectively. Two animals showed scarce cellular infiltrates and inflammation which were graded Banff Borderline, mixed AMR and ACR were found in monkey #10 (Banff IIB) at rejection on POD43. Here neutrophils, mononuclear and activated mononuclear cells (17) were found in glomeruli, PTCs and interstitium of all grafts. There were a total of 4 biopsies taken for cause in monkeys of the intermediate group. In these biopsies we found a delay of the appearance of cellular rejection signs (Banff t, v, and i scores) compared to the BAS-group (Table 3). Furthermore, features of chronic rejection such as vascular intimal thickening increase of mesangial matrix and allograft glomerulopathy began to appear in intermediate rejectors (Figure 5).

Post-transplant humoral response in sensitized recipients after T cell depletion

Retrospective testing revealed that in early rejecting monkeys the level of DSA in their TFXM at the time of transplant seemed similar to intermediate rejectors (MFI ratio 11.5±8.6 vs. 8.3±6.9, p=0.65), whereas in BFXM, DSA were higher in the early rejecting animals (MFI ratio 9.27±1.9 vs. 4.37±2.1, p=0.040; Figure 6A). We were able to measure a significant reduction of DSA within the first 24 hours (48 hours in one case) following reperfusion (Supplemental Figure 2). Animals surviving beyond 5 days experienced a rebound peak in DSA (Figure 6B). The accompanying rise in sCr and BUN correlated with the level of DSA (MFI ratio of BFXM and sCr: correlation coefficient $\rho = 0.71$, p=0.046; BFXM and BUN: correlation coefficient $\rho = 0.72$, $p<0.0001$; Figure 6C). To characterize this rebound further, we investigated post-transplant B cell responses. After transplantation B cell subsets, based on the surface markers shown in Supplemental figure 3, were traced in peripheral blood. Interestingly, in the intermediate rejectors group (n=3) we observed an increase in memory B cells ($CD20^+CD27^+IgD^-$) with a relative reduction of naïve B cells ($CD20^+CD27^-IgD^+$) at 4/5 and 6 weeks after transplantation compared to pretransplant (sensitized) time point (Figure 6D). We did not find this phenomenon in peripheral lymph nodes at necropsy (Supplemental figure 4). Based on the expression of the intracellular marker Ki67, proliferation of memory B cells peaked at weeks 4/5 (Figure 6D).

During T cell repopulation the fraction of both, naïve CD4 and CD8 T cells decreased significantly in peripheral blood and peripheral lymph nodes, giving way to memory phenotypes, primarily CD4 central memory subtype (Figure 7A and B). This phenotypic switching after T cell depletion has been reported (13) using other T cell depleting agents. In order to attribute the germinal center (GC) response to the post-transplant rebound DSA in sensitized animals, we analyzed T follicular helper (Tfh) cells in peripheral lymph nodes defined as $CD4^+PD\text{-}1^{hi}$ cells and GC-Tfh cells defined as $CD4^+PD\text{-}1^{hi}$ $CXCR5^+ICOS^+$ (Figure 7C). We found an increase in percentage of both Tfh cell subtypes in the lymph

nodes at the time of sacrifice in parallel to B memory cell increase in peripheral blood. Finally, we evaluated GCs in situ using antibodies to Ki67, CD3, and CD20 in conjunction with Hoechst staining. At sacrifice, GCs had increased in size and frequency within the B cell follicles of lymph nodes compared to pretransplant time points (Figure 7D). These data suggest that high level of circulating DSA at the time of transplant may rapidly injure the graft and induce hyperacute rejection or acute AMR, while GC-driven DSA-rebound may be responsible for the delayed AMR in sensitized animals.

Discussion

We have established a non-human primate model of AMR with characteristics that parallel those of sensitized human recipients of kidney transplants. Through the use of serial skin transplantation, we have achieved reliable and lasting sensitization levels, as measured by DSA. Following kidney transplantation into these sensitized recipients, rejection occurs with features of acute and hyperacute antibody-mediated injury seen in human transplantation. We therefore believe that this model is highly relevant for testing desensitization treatments using NHP as a relevant preclinical model.

When using induction with IL-2-receptor antagonist basiliximab and standard immunosuppression, rejection was accelerated compared to non-sensitized recipients. Histological changes compatible with AMR were found, and concurrent T cell infiltration occurred within 4 and 8 days in two of three monkeys. We hypothesized that memory T cells induced by skin transplantation contributed to the rejection. Studies have suggested the potential benefits of T cell depleting agents relative to IL-2 receptor blockers in preventing acute rejection in sensitized patients (21–23). In clinical transplantation T cell depletion is widely used in this setting, so for this reason, we introduced T cell depletion in our model. The use of human anti-thymocyte globulin (ATG) in rhesus monkeys is problematic as effects are not equal to those in humans. Alemtuzumab, used off-label in humans, is also not a viable option in most rhesus monkey strains as the main target, CD52, is constitutively expressed on red blood cells (24). We therefore used novel anti-rhesus CD4 and CD8 antibodies to deplete and to better distinguish the effect of DSA. This also provided us a unique opportunity to compare the efficacy of non-depletional vs. depletional induction approaches in sensitized recipients. Not only was survival prolonged, but cellular infiltration was delayed with T cell depletion compared to basiliximab induction.

The observation of thrombotic microangiopathy (TMA) in antibody incompatible grafts is a phenotype of AMR already published in xeno- (25, 26) and human transplantation (27–31). Although calcineurin inhibitors such as tacrolimus can elicit this phenomenon in renal transplants (32–34), given the degree of sensitization, AMR is the most probable cause of TMA since it occurred together with measurable DSA and C4d staining of PTC. Pathophysiologically, TMA in AMR is believed to be caused by antibody binding, endothelial and complement activation and platelet aggregation and does not involve adaptive cellular immunity. We have observed an important phenotype of rejection that may respond well to complement or coagulation targeted therapies.

At later time points, tubulitis was present in addition to changes associated with chronic damage. All 3 intermediate rejectors (DEPL-group) showed changes at least suspicious for cellular rejection in addition to signs of AMR. At this point they had experienced normalization of NK cell numbers in peripheral blood (data not shown) and the T cell repopulation of peripheral blood and lymph nodes showed a predominance of CD4 and CD8 memory cells. Although we conclude that antibodies are the major agent responsible for graft rejection in these cases, the model also affords the opportunity to test novel regimens to specifically address the impact of T cell memory subtypes.

DSA in peripheral blood decreased significantly within the first 24 hours of reperfusion, which is either due to absorption by the graft (35, 36) and/or due to anti-idiotypic antibodies (37). We used BFXM to follow up on DSA after transplantation because anti-CD4 and -CD8 mAb interfered with our TFXM readings. BFXM detects both MHC class I and II antibodies but cannot differentiate between specificities. We found rebound of antibody within the first 10 days after kidney transplantation as seen in humans (11, 38). In 2 animals (early rejectors) this increase coincided with AMR and terminal kidney failure. In 3 animals (intermediate rejectors) sCr and BUN rose but then stabilized, correlating with a decrease in DSA. Burns et al. reported a decrease in DSA in desensitized humans after transplantation (11), but plasmapheresis was performed. In this NHP model, the decrease cannot be attributed to plasmapheresis. It is possible, after initial B memory cell proliferation and differentiation to plasmablasts, that the decrease is a sign of plasmablast exhaustion and the competition for homing to survival niches in the bone marrow to form LLPCs. We found that $CD20^{+}CD27^{+}IgD^{-}$ B cells increased and proliferated in peripheral blood between weeks 1 and weeks 4–6. We attribute this rise to the fact that the monkeys were sensitized. However, we also acknowledge a potential contribution of homeostatic proliferation in response to T cell depletion. Within these time points intermediate rejectors failed. This might be a blueprint of early AMR in clinical transplantation as a second line of immune response in combination with T follicular helper cell proliferation in lymph node germinal centers.

This model provides a platform to address some important aspects relating to sensitized transplant strategies. Novel pretransplant desensitization methods before kidney transplantation, may both allow successful initial transplantation, and reduce the DSA rebound by modulation of the post-transplant germinal center response, including Tfh (39). Additionally early rejection and TMA may be addressed with complement-blockade in the early phase after transplantation (40–42).

Use of this NHP model will allow for combination therapies in a manner highly relevant to human transplantation of the sensitized patient.

Supplementary Material

Refer to Web version on PubMed Central for supplementary material.

Acknowledgments

This work was supported by NIH grant U19AI051731 and NIH grant P51OD11132 in support of Yerkes. CKB received grant support by the Austrian Science Fund (FWF): project J3414 and a research stipend by the Austrian Society of Surgery. The authors would like to thank all collaborators at the Emory Transplant Center and at the Yerkes Primate Research Center, especially all veterinary technicians and pathology lab staff. Special thanks to Sebastian Perez for help with statistics, Yerkes veterinarians Elizabeth Strobert and Joe Jenkins and Eileen Breding and Anapatricia Garcia for their help with electron microscopy.

Abbreviations

ATG	anti-thymocyte globulin
AMR	antibody-mediated rejection
ACR	acute cellular rejection
BFXM	B cell flow cytometry crossmatch
BUN	blood urea nitrogen
cg	allograft glomerulopathy (Banff score)
ci	interstitial fibrosis (Banff score)
ct	tubular atrophy (Banff score)
cv	vascular fibrous intimal thickening (Banff score)
D	day
DSA	Donor specific antibody
FXM	flow cytometry crossmatch
g	glomerulitis (Banff score)
IA	immunoadsorption
mAb	monoclonal antibody
MFI	mean fluorescence intensity
MHC	major histocompatibility complex
mm	mesangial matrix increase (Banff score)
MST	mean survival time
NHP	non-human primates
POD	post-operative day
PP	plasmapheresis
PTC	peritubular capillary
ptc	peritubular capillary inflammation (Banff score)
rhCMV	rhesus cytomegalovirus
sCr	serum creatinine

TFXM	T cell flow cytometry crossmatch
TMA	thrombotic microangiopathy

References

1. Matas AJ, Smith JM, Skeans MA, Thompson B, Gustafson SK, Schnitzler MA, et al. OPTN/SRTR 2012 Annual Data Report: Kidney. Am J Transplant. 2013; 14(S1):1–44.
2. Eurotransplant International Foundation; 2014 May 17. ANNUAL REPORT 2013. http://www.eurotransplant.org: Report No
3. Vo AA, Sinha A, Haas M, Choi J, Mirocha J, Kahwaji J, et al. Factors Predicting Risk for Antibody-mediated Rejection and Graft Loss in Highly Human Leukocyte Antigen Sensitized Patients Transplanted After Desensitization. Transplantation. 2015; 99(7):1423–1430. [PubMed: 25606792]
4. Cecka JM, Kucheryavaya AY, Reinsmoen NL, Leffell MS. Calculated PRA: initial results show benefits for sensitized patients and a reduction in positive crossmatches. Am J Transplant. 2011; 11(4):719–724. [PubMed: 21114658]
5. Israni AK, Salkowski N, Gustafson S, Snyder JJ, Friedewald JJ, Formica RN, et al. New national allocation policy for deceased donor kidneys in the United States and possible effect on patient outcomes. J Am Soc Nephrol. 2014; 25(8):1842–1848. [PubMed: 24833128]
6. Montgomery RA, Lonze BE, King KE, Kraus ES, Kucirka LM, Locke JE, et al. Desensitization in HLA-incompatible kidney recipients and survival. N Engl J Med. 2011; 365(4):318–326. [PubMed: 21793744]
7. Sharif A, Kraus ES, Zachary AA, Lonze BE, Nazarian SM, Segev DL, et al. Histologic phenotype on 1-year posttransplantation biopsy and allograft survival in HLA-incompatible kidney transplants. Transplantation. 2014; 97(5):541–547. [PubMed: 24521779]
8. Bagnasco SM, Zachary AA, Racusen LC, Arend LJ, Carter-Monroe N, Alachkar N, et al. Time course of pathologic changes in kidney allografts of positive crossmatch HLA-incompatible transplant recipients. Transplantation. 2014; 97(4):440–445. [PubMed: 24531821]
9. Orandi BJ, Garonzik-Wang JM, Massie AB, Zachary AA, Montgomery JR, Van Arendonk KJ, et al. Quantifying the risk of incompatible kidney transplantation: a multicenter study. Am J Transplant. 2014; 14(7):1573–1580. [PubMed: 24913913]
10. Bentall A, Cornell LD, Gloor JM, Park WD, Gandhi MJ, Winters JL, et al. Five-year outcomes in living donor kidney transplants with a positive crossmatch. Am J Transplant. 2013; 13(1):76–85. [PubMed: 23072543]
11. Burns JM, Cornell LD, Perry DK, Pollinger HS, Gloor JM, Kremers WK, et al. Alloantibody levels and acute humoral rejection early after positive crossmatch kidney transplantation. Am J Transplant. 2008; 8(12):2684–2694. [PubMed: 18976305]
12. Archdeacon P, Chan M, Neuland C, Velidedeoglu E, Meyer J, Tracy L, et al. Summary of FDA Antibody-Mediated Rejection Workshop. Am J Transplant. 2011; 11(5):896–906. [PubMed: 21521465]
13. Page EK, Page AJ, Kwun J, Gibby AC, Leopardi F, Jenkins JB, et al. Enhanced de novo alloantibody and antibody-mediated injury in rhesus macaques. Am J Transplant. 2012; 12(9): 2395–2405. [PubMed: 22776408]
14. Haas M, Sis B, Racusen LC, Solez K, Glotz D, Colvin RB, et al. Banff 2013 meeting report: inclusion of c4d-negative antibody-mediated rejection and antibody-associated arterial lesions. Am J Transplant. 2014; 14(2):272–283. [PubMed: 24472190]
15. Welch BL. The generalisation of student's problems when several different population variances are involved. Biometrika. 1947; 34(1–2):28–35. [PubMed: 20287819]
16. Bland JM, Altman DG. Calculating correlation coefficients with repeated observations: Part 1--Correlation within subjects. BMJ. 1995; 310(6977):446. [PubMed: 7873953]
17. Colvin RB, Cohen AH, Saiontz C, Bonsib S, Buick M, Burke B, et al. Evaluation of pathologic criteria for acute renal allograft rejection: reproducibility, sensitivity, and clinical correlation.

Journal of the American Society of Nephrology : JASN. 1997; 8(12):1930–1941. [PubMed: 9402096]

18. Mavilio D, Benjamin J, Kim D, Lombardo G, Daucher M, Kinter A, et al. Identification of NKG2A and NKp80 as specific natural killer cell markers in rhesus and pigtailed monkeys. Blood. 2005; 106(5):1718–1725. [PubMed: 15899917]
19. Autissier P, Soulas C, Burdo TH, Williams KC. Immunophenotyping of lymphocyte, monocyte and dendritic cell subsets in normal rhesus macaques by 12-color flow cytometry: clarification on DC heterogeneity. J Immunol Methods. 2010; 360(1–2):119–128. [PubMed: 20600075]
20. Pereira LE, Johnson RP, Ansari AA. Sooty mangabeys and rhesus macaques exhibit significant divergent natural killer cell responses during both acute and chronic phases of SIV infection. Cell Immunol. 2008; 254(1):10–19. [PubMed: 18640666]
21. Anglicheau D, Loupy A, Suberbielle C, Zuber J, Patey N, Noel LH, et al. Posttransplant prophylactic intravenous immunoglobulin in kidney transplant patients at high immunological risk: a pilot study. Am J Transplant. 2007; 7(5):1185–1192. [PubMed: 17359509]
22. Hellemans R, Hazzan M, Durand D, Mourad G, Lang P, Kessler M, et al. Daclizumab Versus Rabbit Antithymocyte Globulin in High-Risk Renal Transplants: Five-Year Follow-up of a Randomized Study. Am J Transplant. 2015
23. Brokhof MM, Sollinger HW, Hager DR, Muth BL, Pirsch JD, Fernandez LA, et al. Antithymocyte globulin is associated with a lower incidence of de novo donor-specific antibodies in moderately sensitized renal transplant recipients. Transplantation. 2014; 97(6):612–617. [PubMed: 24531846]
24. van der Windt DJ, Smetanka C, Macedo C, He J, Lakomy R, Bottino R, et al. Investigation of lymphocyte depletion and repopulation using alemtuzumab (Campath-1H) in cynomolgus monkeys. Am J Transplant. 2010; 10(4):773–783. [PubMed: 20420638]
25. Shimizu A, Meehan SM, Kozlowski T, Sablinski T, Ierino FL, Cooper DK, et al. Acute humoral xenograft rejection: destruction of the microvascular capillary endothelium in pig-to-nonhuman primate renal grafts. Lab Invest. 2000; 80(6):815–830. [PubMed: 10879733]
26. Shimizu A, Yamada K, Robson SC, Sachs DH, Colvin RB. Pathologic characteristics of transplanted kidney xenografts. J Am Soc Nephrol. 2012; 23(2):225–235. [PubMed: 22114174]
27. Satoskar AA, Pelletier R, Adams P, Nadasdy GM, Brodsky S, Pesavento T, et al. De novo thrombotic microangiopathy in renal allograft biopsies-role of antibody-mediated rejection. Am J Transplant. 2010; 10(8):1804–1811. [PubMed: 20659088]
28. Noris M, Remuzzi G. Thrombotic microangiopathy after kidney transplantation. Am J Transplant. 2010; 10(7):1517–1523. [PubMed: 20642678]
29. Halloran PF, Schlaut J, Solez K, Srinivasa NS. The significance of the anti-class I response. II. Clinical and pathologic features of renal transplants with anti-class I-like antibody. Transplantation. 1992; 53(3):550–555. [PubMed: 1549846]
30. Vo AA, Sinha A, Haas M, Choi J, Mirocha J, Kahwaji J, et al. Factors Predicting Risk for Antibody-Mediated Rejection and Graft Loss in Highly Human Leukocyte Antigen Sensitized Patients Transplanted After Desensitization. Transplantation. 2015
31. Racusen LC, Haas M. Antibody-mediated rejection in renal allografts: lessons from pathology. Clin J Am Soc Nephrol. 2006; 1(3):415–420. [PubMed: 17699240]
32. Randhawa PS, Tsamandas AC, Magnone M, Jordan M, Shapiro R, Starzl TE, et al. Microvascular changes in renal allografts associated with FK506 (Tacrolimus) therapy. Am J Surg Pathol. 1996; 20(3):306–312. [PubMed: 8772784]
33. Young BA, Marsh CL, Alpers CE, Davis CL. Cyclosporine-associated thrombotic microangiopathy/hemolytic uremic syndrome following kidney and kidney-pancreas transplantation. Am J Kidney Dis. 1996; 28(4):561–571. [PubMed: 8840947]
34. Zarifian A, Meleg-Smith S, O'Donovan R, Tesi RJ, Batuman V. Cyclosporine-associated thrombotic microangiopathy in renal allografts. Kidney Int. 1999; 55(6):2457–2466. [PubMed: 10354295]
35. Martin L, Guignier F, Mousson C, Rageot D, Justrabo E, Rifle G. Detection of donor-specific anti-HLA antibodies with flow cytometry in eluates and sera from renal transplant recipients with chronic allograft nephropathy. Transplantation. 2003; 76(2):395–400. [PubMed: 12883199]

36. Adeyi OA, Girnita AL, Howe J, Marrari M, Awadalla Y, Askar M, et al. Serum analysis after transplant nephrectomy reveals restricted antibody specificity patterns against structurally defined HLA class I mismatches. Transpl Immunol. 2005; 14(1):53–62. [PubMed: 15814283]

37. Hardy MA, Suciu-Foca N, Reed E, Benvenisty AI, Smith C, Rose E, et al. Immunomodulation of kidney and heart transplants by anti-idiotypic antibodies. Ann Surg. 1991; 214(4):522–528. discussion 8–30. [PubMed: 1953103]

38. Jackson AM, Kraus ES, Orandi BJ, Segev DL, Montgomery RA, Zachary AA. A closer look at rituximab induction on HLA antibody rebound following HLA-incompatible kidney transplantation. Kidney Int. 2015; 87(2):409–416. [PubMed: 25054778]

39. Kim EJ, Kwun J, Gibby AC, Hong JJ, Farris AB 3rd, Iwakoshi NN, et al. Costimulation blockade alters germinal center responses and prevents antibody-mediated rejection. Am J Transplant. 2014; 14(1):59–69. [PubMed: 24354871]

40. Stegall MD, Diwan T, Raghavaiah S, Cornell LD, Burns J, Dean PG, et al. Terminal complement inhibition decreases antibody-mediated rejection in sensitized renal transplant recipients. Am J Transplant. 2011; 11(11):2405–2413. [PubMed: 21942930]

41. Locke JE, Magro CM, Singer AL, Segev DL, Haas M, Hillel AT, et al. The use of antibody to complement protein C5 for salvage treatment of severe antibody-mediated rejection. Am J Transplant. 2009; 9(1):231–235. [PubMed: 18976298]

42. Tillou X, Poirier N, Le Bas-Bernardet S, Hervouet J, Minault D, Renaudin K, et al. Recombinant human C1-inhibitor prevents acute antibody-mediated rejection in alloimmunized baboons. Kidney Int. 2010; 78(2):152–159. [PubMed: 20336054]

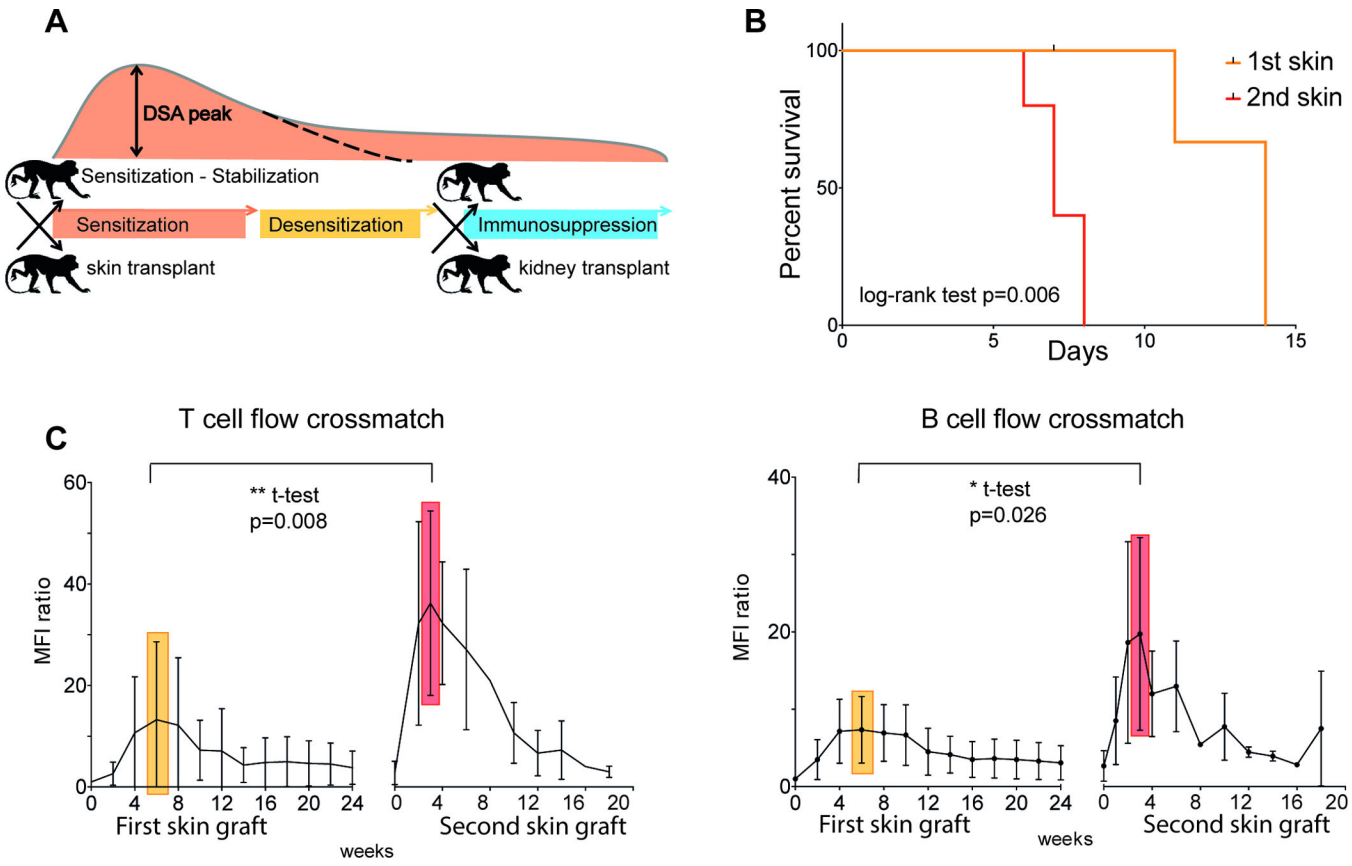

Figure 1. Sensitization by skin transplants and course of DSA

(A) Model scheme: skin transplant for sensitization; planned desensitization after stabilization of DSA level; kidney transplant to prove efficacy of therapy using clinically relevant immunosuppression. B) Survival time of first and second skin grafts (n=5 in each group). C) T cell/B cell FXM of recipient serum with donor T/B cells at serial time points after first (n=11) and second (n=7) skin graft. Results are expressed as MFI ratio to baseline. The mean maximum was reached at week 6 (yellow) and 3 (red) respectively. The mean peak after second skin graft was significantly higher (t-test with Welch correction for unequal variances). DSA, Donor specific antibody; FXM, flow cytometry crossmatch; MFI, mean fluorescence intensity;

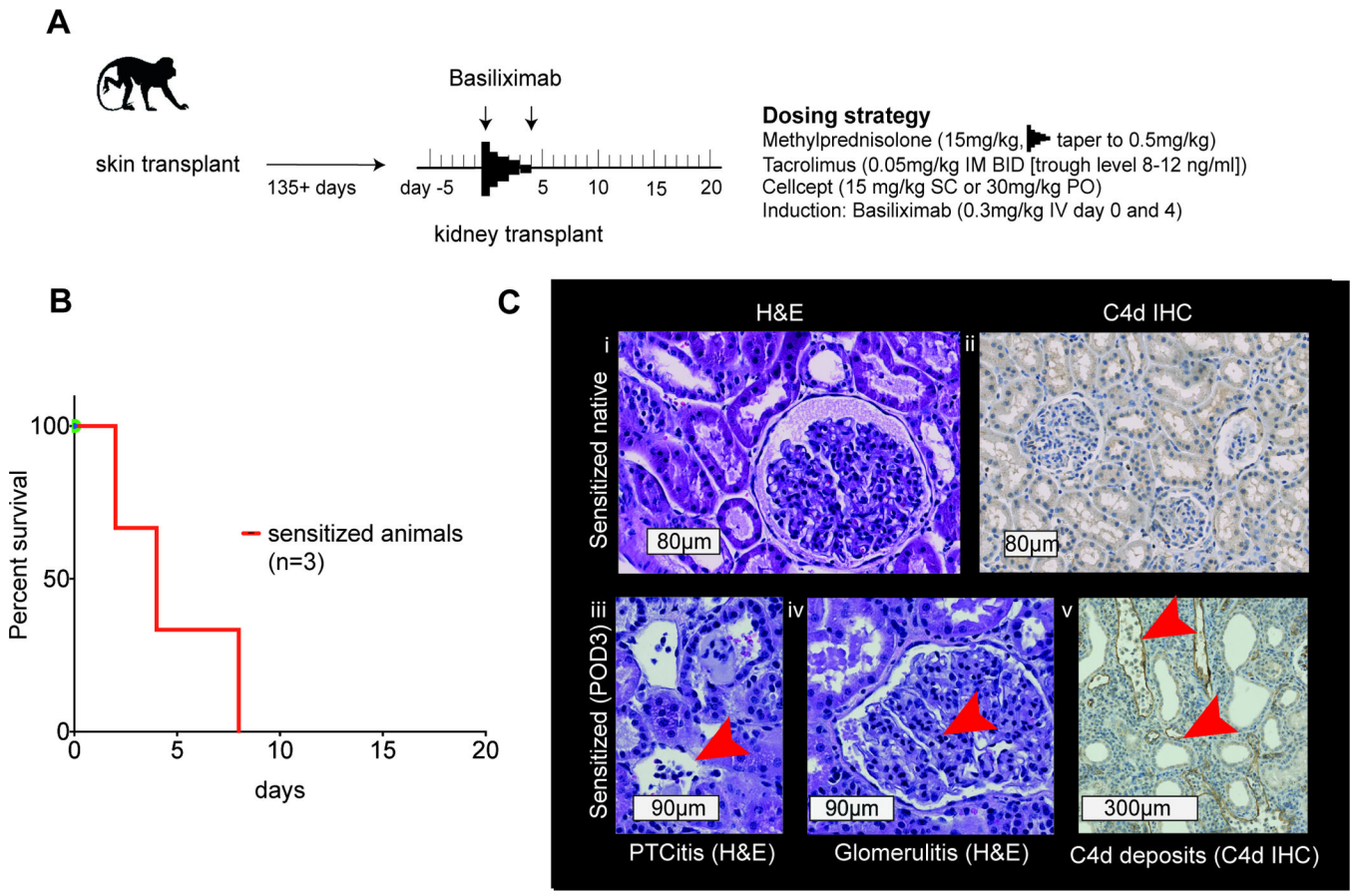

Figure 2. Kidney transplants in sensitized NHP with basiliximab induction - BAS-group

A) Scheme and dosing strategy; B) Survival of sensitized animals after kidney transplant with basiliximab induction; C) (text boxes represent scale bars): i) native kidney from sensitized animal (H&E); ii) C4d negative native kidney from sensitized animal. Features of rejection: iii) peritubular capillaritis (H&E, arrow at inflammatory cells in PTC); iv) glomerulitis (H&E, arrow at inflammatory cell in capillary); v) C4d staining of peritubular capillaries (arrows at staining of C4d deposition in PTC wall). NHP, nonhuman primates; mAb, monoclonal antibody; PTC, peritubular capillary

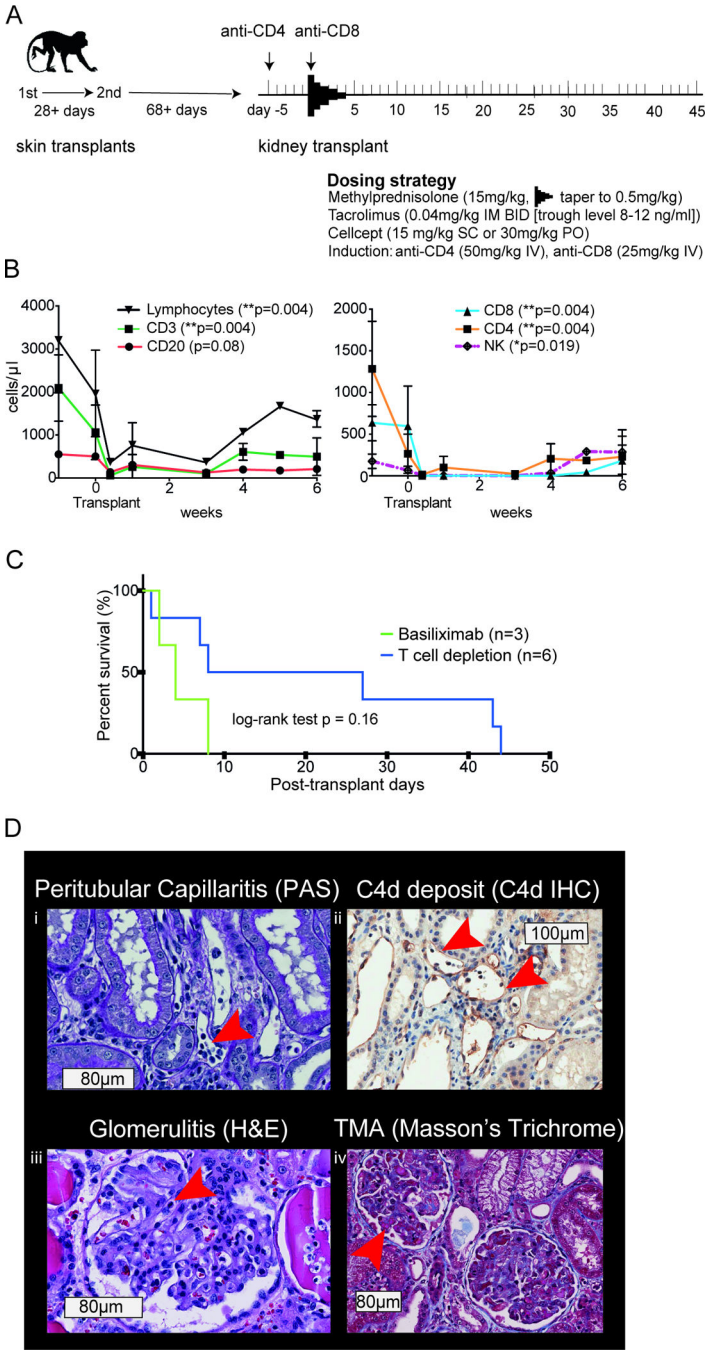

Figure 3. Kidney transplants in sensitized NHP with T cell depleting rhesus anti-CD4 and anti-CD8 mAb induction - DEPL-group

A) Scheme and dosing strategy. B) Numbers of lymphocytes, T, B and NK cells after depletion with anti-CD4 and anti-CD8 antibodies (p-values show differences at time points prior and the first week after depletion; paired t-test). C) Mean survival time after depletion compared to basiliximab induction. D) (boxes represent scale bars): Histologic phenotype after rejection: i) peritubular capillaritis (PAS, arrow at inflammatory cells in PTC); ii) C4d staining of peritubular capillaries (arrows at staining of C4d deposition in PTC wall); iii) glomerulitis (H&E, arrow at inflammatory cell in capillary); iv) thrombotic microangiopathy

[TMA] (Masson's Trichrome, arrow at fibrin thrombi). NHP, nonhuman primates; mAb, monoclonal antibody; PTC, peritubular capillary

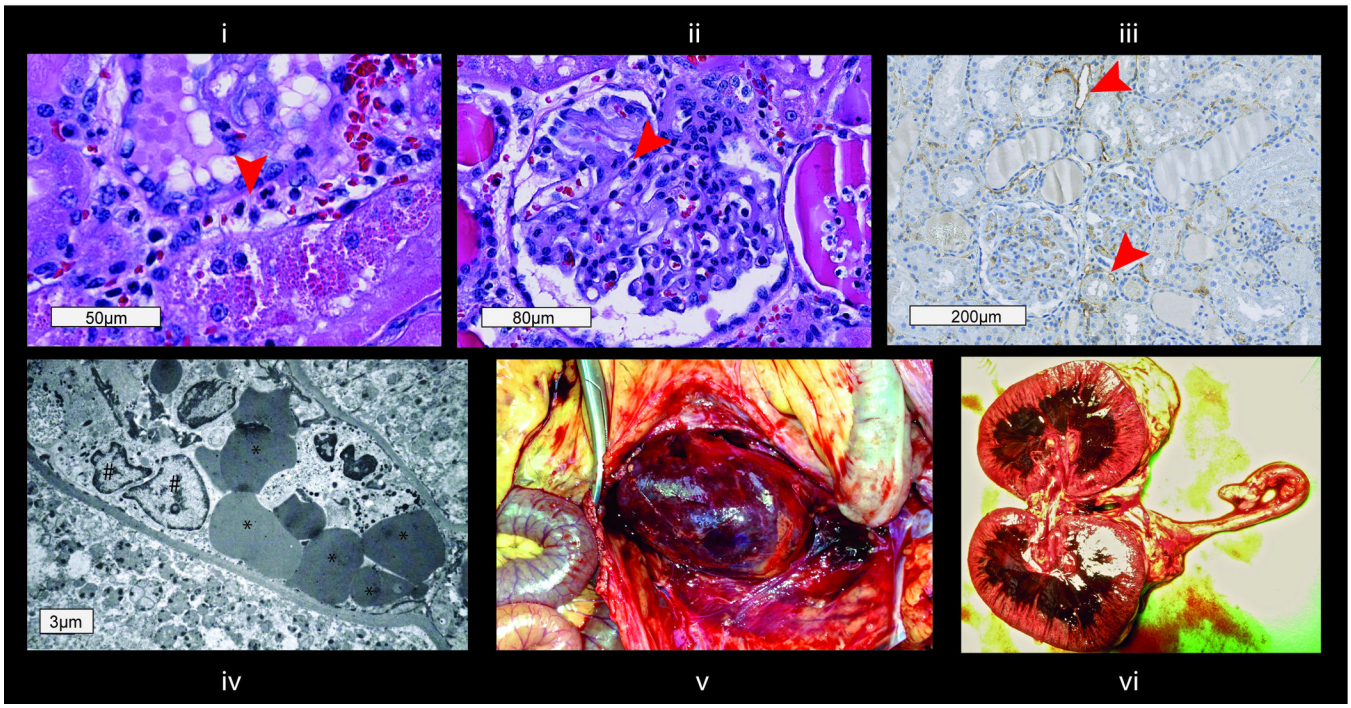

Figure 4. Phenotype after hyperacute rejection (boxes represent scale bars)

i) Peritubular capillaritis (H&E, arrow at inflammatory cells in PTC); ii) glomerulitis (H&E, arrow at inflammatory cell in capillary); iii) C4d staining of peritubular capillaries (arrows at staining of C4d deposition in PTC wall); iv) electron microscopy image with inflammatory cells (#), erythrocytes (*) and detritus in the peritubular space; v) hemorrhagic graft around 22 hours after perfusion. ptc, peritubular capillary inflammation (Banff score);

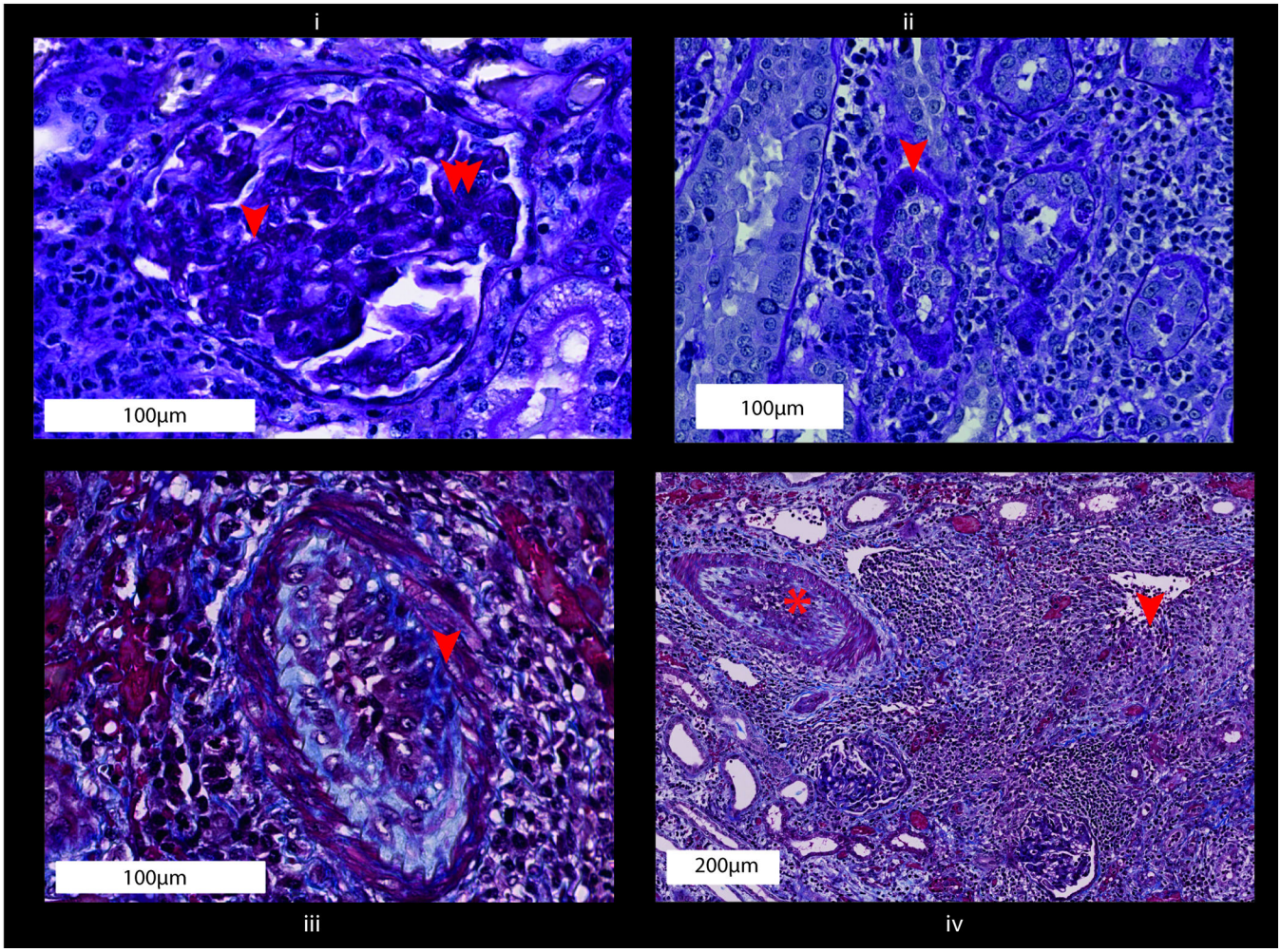

Figure 5. Histological features in T cell depleted (DEPL-group) intermediate rejectors compatible with chronic rejection as established by Banff score (boxes represent scale bars)

(i) Glomerular basement membrane duplication is compatible with cg1 glomerulopathy (arrow); Mesangial expansion was present in some glomeruli, considered mm1 for purposes of Banff scoring (double arrow) (PAS). (ii) Focal tubular atrophy was present, compatible with a Banff ct1 score (PAS). (iii) Arteritis is superimposed upon arterial intimal thickening leading to at least moderate stenosis of the arterial lumen, considered cv2 for purposes of Banff scoring (Trichrome). (iv) Areas of interstitial fibrosis/scarring are present, considered Banff ci1 overall (arrow), accompanied by admixed tubular atrophy and adjacent arteritis (*) (Trichrome). cg, allograft glomerulopathy (Banff score); mm, mesangial matrix increase (Banff score); cv, vascular fibrous intimal thickening (Banff score); ci, interstitial fibrosis (Banff score).

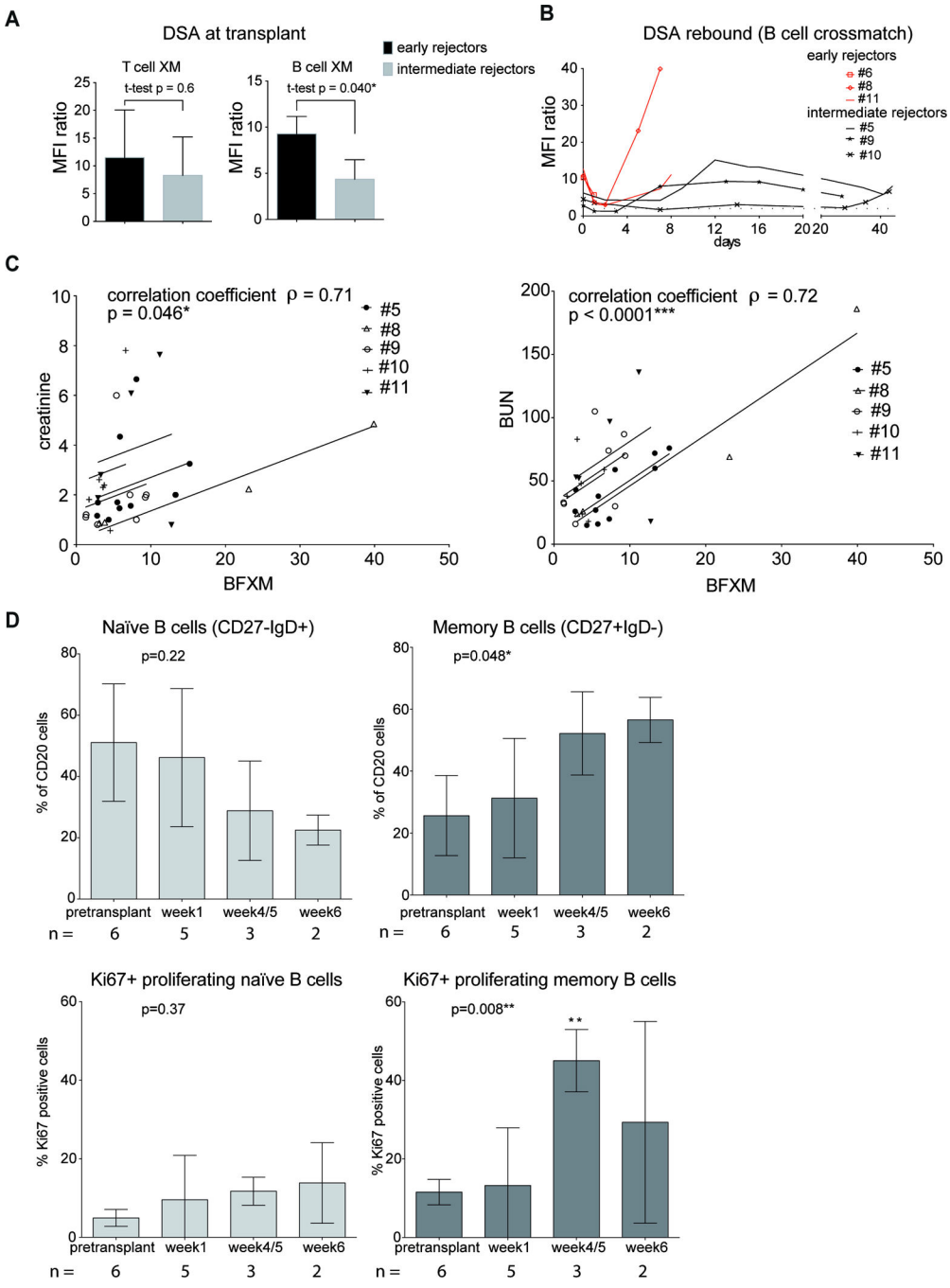

Figure 6. Posttransplant DSA, correlation with kidney function and memory B cells in sensitized NHP with T cell depleting induction - DEPL-group (for gating strategy see Supplemental figure 3)

(A) DSA level at transplant, early (n=3)versus intermediate (n=3) rejectors: early rejectors were found to have higher DSA at transplant than intermediate rejectors in B cell flow crossmatch (BFXM), no significant difference in T cell flow crossmatch (TFXM). B) DSA course over posttransplant period, curve ends at sacrifice; early rejectors in red: DSA rebound was common within days after transplantation, early rejectors failed at the first peak. C) Correlation of BFXM with creatinine and BUN readings (linear model; BFXM vs.

serum creatinine and BUN respectively: parallel lines fitted for each subject): increase/decrease in DSA measured by BFXM were well correlated with increases/decreases in serum creatinine and BUN. D) Changes in proportions of naïve ($CD20^+CD27^-IgD^+$) and memory ($CD20^+CD27^+IgD^-$) B cell subtypes and Ki67 marker expression in these subtypes posttransplant (one-way ANOVA with Dunnett's test; * significance in Dunnett's test). Memory B cells increased at the cost of naïve B cells posttransplant, a maximum in proliferation by Ki67-expression was found at time point week 4/5. N, number of monkeys available for analysis; DSA, Donor specific antibody; NHP, nonhuman primates; BUN, blood urea nitrogen.

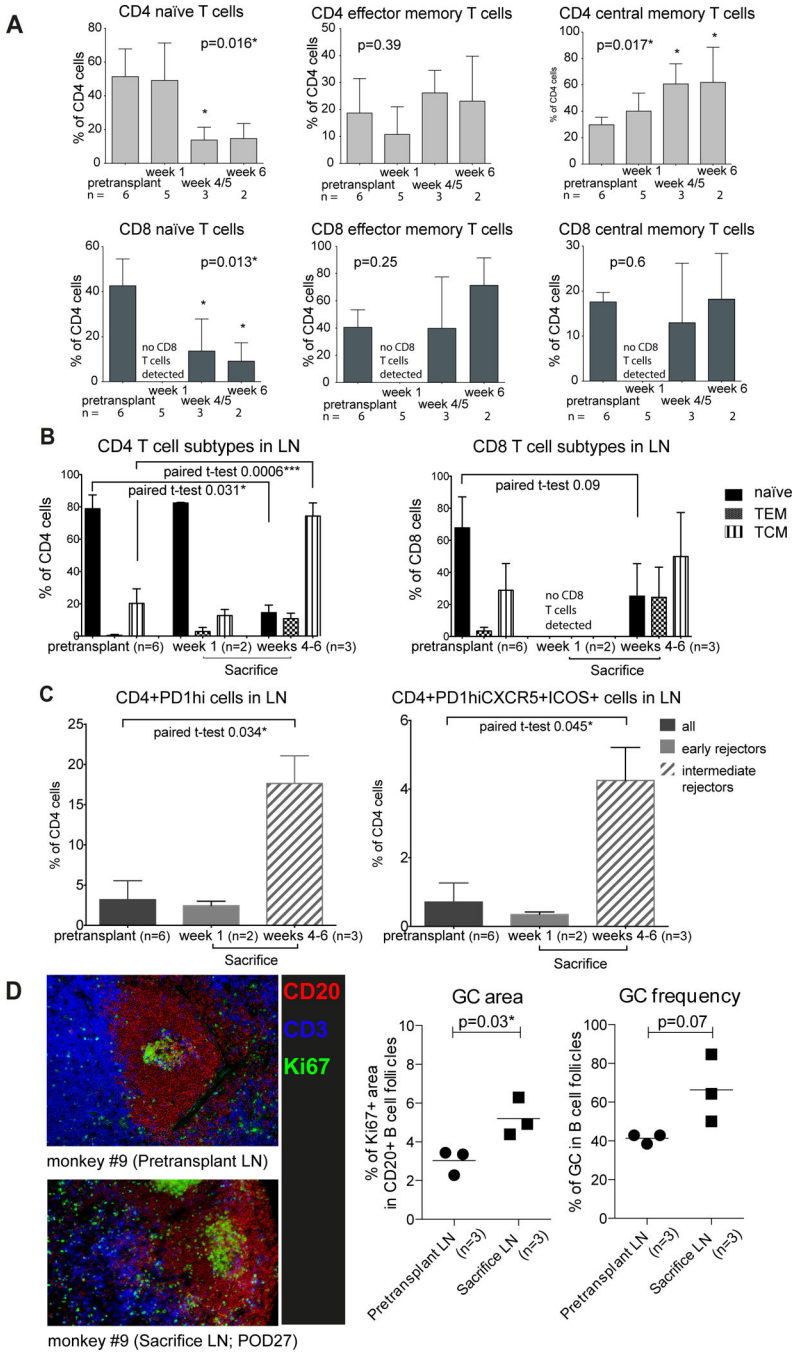

Figure 7. T cell subtypes and T follicular helper cells in sensitized NHP with T cell depleting induction - DEPL-group (for gating strategy see Figure S3)

(A) Reconstitution of T cell repertoire in peripheral blood after T cell depletion: shift from naïve cells to memory cell subtypes (one-way ANOVA with Dunnett's test; *significance in Dunnett's test; week 1 was excluded in CD8 analysis due to lack of cells). (B) T cell subtypes in lymph nodes pretransplant and at sacrifice: reconstitution favored memory cell subtypes at 4–6 weeks. (C) Comparison of $CD4^{+}PD1^{high}$ cells and $CD4^{+}PD1^{high}CXCR5^{+}ICOS^{+}$ cells between pretransplant and sacrifice time points in lymph nodes; week 1: no change in early rejectors, week 4–6: increase in intermediate rejectors.

(D) Germinal center staining: in B cell follicles germinal center area and frequency increased at sacrifice compared to the pretransplant time point (t-test). N, number of monkeys available for analysis; NHP, non-human primates.

Table 1

Results of sensitized monkeys after Basiliximab induction

Animal	DSA T cell XM (MFI ratio)		DSA B cell XM (MFI ratio)		Survival (days)	ACR	AMR score (Banff)				Histologic interpretation
	highest	at transplant	highest	at transplant			g	ptc	C4d	total	
Monkey #2	5.4	2.1	2.8	1.8	1	none	0	0	0	**0**	no rejection (excluded)
Monkey #4	34.5	3.5	13.4	3.7	2	none	2	0	0	**2**	susp. AMR, C4d negative
Monkey #1	63.8	3.5	5.7	2.8	4	Banff IIA	3	2	1	**6**	AMR + ACR
Monkey #3	8.4	1.2	5.9	1.5	8	Banff III	3	1	2	**6**	AMR + ACR

Abbreviations: MFI ratio: MFI fold increase to baseline level; ACR: acute cellular rejection; AMR: antibody-mediated rejection; Banff-Score: g: glomerulitis, ptc: peritubular capillary inflammation, C4d: C4d deposition in walls of peritubular capillaries (immunohistochemistry); susp.: suspected

Table 2

Results of sensitized monkeys after induction with T cell depleting anti-CD4 and anti-CD8

Animal	DSA T cell XM (MFI ratio)		DSA B cell XM (MFI ratio)		Survival (days)	ACR	AMR score (Banff)				Histologic interpretation
	highest	at transplant	highest	at transplant			g	ptc	C4d	total	
Monkey #6	75.1	21.4	45.5	8.6	1	none	2	2	2	**6**	AMR, TMA, hyperacute
Monkey #7	26.3	8.2	15.9	5.1	3	none	0	1	1	**2**	no rejection (excluded)
Monkey #8	28.9	6.2	34.4	7.8	7	none	3	0	2	**5**	AMR, TMA
Monkey #11	10.2	6.8	17.3	11.4	8	none	3	1	2	**6**	AMR, TMA
Monkey #9	18.6	2.9	9.4	2.2	27	Borderline	3	1	2	**6**	AMR, borderline ACR
Monkey #10	44.3	16.1	18.7	4.5	43	Banff IIB	3	2	2	**7**	AMR + ACR
Monkey #5	52.7	5.9	19.8	6.4	44	Borderline	1	2	3	**6**	AMR, borderline ACR

Abbreviations: MFI ratio: MFI fold increase to baseline level; ACR: acute cellular rejection; AMR: antibody-mediated rejection; Banff-Score: g: glomerulitis, ptc: peritubular capillary inflammation, C4d: C4d deposition in walls of peritubular capillaries (immunohistochemistry)

Table 3

Comparison of histologic findings in necropsy kidney graft specimens of BAS-monkeys and in for-cause biopsies of DEPL-monkeys

Group	Animal #	POD	specimen	Banff t score	Banff v score	Banff i score
BAS	Monkey #4	2	graft	0	0	0
	Monkey #1	4	graft	2	1	3
	Monkey #3	8	graft	3	3	3
DEPL	Monkey #9	13	biopsy	0	0	0
	Monkey #10	24	biopsy	0	0	0
	Monkey #5	8	biopsy	0	0	0
	Monkey #5	35	biopsy	1	0	1

Abbreviations: BAS: group receiving Basiliximab induction; DEPL: group receiving T-cell depletional induction; POD: post operative day; Banff score: t: tubulitis; intimal arteritis; i: mononuclear cell interstitial inflammation